

Energy-Efficient Extended Sub-connected Architecture for Hybrid Precoding in Millimeter Wave Massive MIMO Systems

Yun Chen*, Da Chen*, and Tao Jiang*

*School of Electronics Information and Communications, Huazhong University of Science and Technology, China
Email: chen_yun@hust.edu.cn; chenda@hust.edu.cn; Tao.Jiang@ieee.org

Abstract—In this paper, we propose an extended sub-connected architecture with arbitrary radio frequency (RF) and antenna mappings (i.e., the number of RF chains connected to a subarray and the number of antennas in each subarray can be arbitrary) to improve the energy efficiency of the hybrid precoding in millimeter wave massive multiple input multiple output (MIMO) systems. For any given RF and antenna mappings in this extended sub-connected architecture, we propose a successive interference cancelation based hybrid precoding scheme with near-optimal performance. This scheme firstly decomposes the total achievable rate optimization problem into multiple sub-rate optimization problems each of which is only related to one subarray, then, maximizes these sub-rates successively. Simulation results demonstrate that the proposed scheme achieves similar achievable rate as the corresponding unconstraint optimal precoding scheme and the energy efficiency of the proposed scheme in the extended sub-connected architecture is the best compared with the existing schemes in the full-connected and sub-connected architectures.

Index Terms—MIMO, millimeter wave communications, hybrid precoding, energy-efficient.

I. INTRODUCTION

The combination of millimeter wave and massive multiple input multiple output (MIMO) is considered as one of the promising candidate technologies for the next 5G communication systems due to the large bandwidth and high spectral efficiency [1]. On the one hand, the small wave length of millimeter wave make it possible to pack a large number of antennas in a compact area. On the other hand, the large antenna array could provide significant precoding gains to compensate for the high path loss of millimeter wave signals [2]. However, the precoding is usually realized in the digital domain and requires radio frequency (RF) comparable in number to the antennas in traditional MIMO systems [3]–[5]. The digital precoding will bring prohibitive energy consumption in millimeter wave massive MIMO systems with large antenna arrays. To solve this problem, the hybrid precoding is proposed, where signals are firstly precoded by a low-dimensional digital precoder to cancel the interference and allocate power, then, precoded by a high-dimensional analog precoder to produce high antenna gains [6].

Most hybrid precoding schemes consider the full-connected and the sub-connected architectures. In the full-connected architecture, each RF chain is connected to all antennas by large number of phase shifters to obtain full precoding gains, which also leads to high energy consumption [7]. The sub-connected

architecture requires smaller number of phase shifters, but causes some visible performance loss [8]. Therefore, in terms of energy efficiency, the best hybrid precoding architecture is still unknown. More recently, a more general sub-connected architecture, named as hybridly-connected architecture, was proposed, where each sub-array could be connected to multiple RF chains [9]. However, the hybridly-connected architecture assumes the numbers of RF chains for all subarrays are the same, which still limits the degree of freedom to obtain better energy efficient architecture.

In this paper, we propose an extended sub-connected architecture, where the number of RF chains connected to a subarray and the number of antennas in each subarray can be arbitrary, to improve the energy efficiency of the hybrid precoding in millimeter wave massive MIMO systems. Under different RF and antenna mappings, the structure of the hybrid precoding and the total power consumption are different. For any given RF and antenna mappings, a successive interference cancelation (SIC) based hybrid precoding scheme with near-optimal performance is proposed. This scheme firstly decomposes the total achievable rate optimization problem into multiple sub-rate optimization problems each of which is only related to one subarray, then, maximizes these sub-rates successively. Simulation results demonstrate that the proposed scheme achieves similar achievable rate as the corresponding unconstraint optimal precoding scheme and the energy efficiency of the proposed scheme in the extended sub-connected architecture is the best compared with the existing schemes in the full-connected and sub-connected architectures.

Notation: a and A are scalars, \mathbf{a} is a vector, and \mathbf{A} is a matrix. $\|\mathbf{a}\|_2$ is the l_2 norm of \mathbf{a} and $\|\mathbf{A}\|_F$ is the Frobenius norm of \mathbf{A} . \mathbf{A}^T , \mathbf{A}^* , \mathbf{A}^{-1} and $|\mathbf{A}|$ denote the transpose, conjugate transpose, inverse, and determinant of \mathbf{A} , respectively. \mathbf{I}_N denotes a $N \times N$ identity matrix. $\mathbb{E}[\cdot]$ denotes the expectation.

II. SYSTEM MODEL AND CHANNEL MODEL

We consider a single user millimeter wave massive MIMO system, where the transmitter is equipped with N_t antennas and N_{RF}^t RF chains. N_s data streams are transmitted to the receiver with N_r antennas and N_{RF}^r RF chains. The received $N_r \times 1$ signal vector \mathbf{y} can be presented as

$$\mathbf{y} = \sqrt{\rho} \mathbf{H} \mathbf{F}_{\text{RF}} \mathbf{F}_{\text{BBS}} + \mathbf{n}, \quad (1)$$

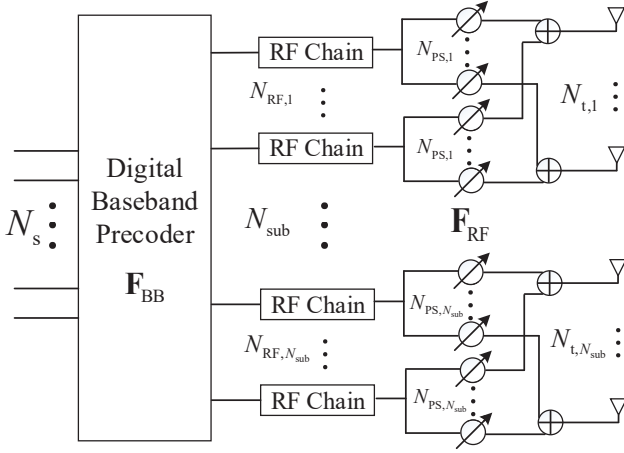


Fig. 1. The extended sub-connected architecture for hybrid precoding.

where ρ is the average received power, \mathbf{H} is the $N_r \times N_t$ millimeter wave channel matrix, \mathbf{F}_{RF} of size $N_t \times N_{\text{RF}}^t$ is the analog precoding matrix, \mathbf{F}_{BB} of size $N_{\text{RF}} \times N_s$ is the baseband precoding matrix, \mathbf{s} is the $N_s \times 1$ signal vector with $\mathbb{E}[\mathbf{s}\mathbf{s}^*] = \frac{1}{N_s} \mathbf{I}_{N_s}$, and \mathbf{n} is the vector of independent and identically distributed (i.i.d.) $\mathcal{CN}(0, \sigma_n^2)$ noise.

Since the limited spatial scattering of millimeter wave signals, the geometric Saleh-Valenzuela model is usually used to represent the millimeter wave channel, which is given by

$$\mathbf{H} = \sqrt{\frac{N_t N_r}{N_{\text{cl}} N_{\text{ray}}}} \sum_{m=1}^{N_{\text{cl}}} \sum_{n=1}^{N_{\text{ray}}} \alpha_{m,n} \mathbf{a}_r(\theta_{m,n}^r) \mathbf{a}_t^*(\theta_{m,n}^t), \quad (2)$$

where N_{cl} is the number of scattering clusters and each cluster contributes N_{ray} propagation paths, $\alpha_{m,n}$ denotes the complex gain of the n_{th} path in the m_{th} cluster, $\theta_{m,n}^r \in (0, 2\pi]$ and $\theta_{m,n}^t \in (0, 2\pi]$ are the AOA and AOD, respectively. For the typical uniform linear arrays (ULAs) equipped at both the transmitter and the receiver, we have

$$\mathbf{a}_t(\theta_{m,n}^t) = \frac{1}{\sqrt{N_t}} \begin{bmatrix} 1, e^{j(2\pi/\lambda)d\sin(\theta_{m,n}^t)}, \dots, e^{j(N_t-1)(2\pi/\lambda)d\sin(\theta_{m,n}^t)} \end{bmatrix}^T, \quad (3)$$

$$\mathbf{a}_r(\theta_{m,n}^r) = \frac{1}{\sqrt{N_r}} \begin{bmatrix} 1, e^{j(2\pi/\lambda)d\sin(\theta_{m,n}^r)}, \dots, e^{j(N_r-1)(2\pi/\lambda)d\sin(\theta_{m,n}^r)} \end{bmatrix}^T, \quad (4)$$

where λ is the signal wavelength and $d = \lambda/2$ denotes the aperture domain sample spacing.

III. ENERGY EFFICIENT HYBRID PRECODING

In this section, we first describe the structure of the considered extended sub-connected architecture. Then, we propose a SIC-based hybrid precoding scheme in this architecture with arbitrary antenna and RF mappings.

A. The extended sub-connected architecture

Fig. 1 shows the transmitter of the extended sub-connected architecture and the receiver is symmetrical with the transmitter. In the extended sub-connected architecture, the number of RF chains connected to a subarray and the number of antennas in each subarray can be arbitrary, where the number of the subarray is N_{sub} , $N_{\text{RF},i}$ and $N_{t,i}$, $i = 1, 2, \dots, N_{\text{sub}}$ denote the number of RF chains and antennas connected to the i_{th} subarray, respectively, $N_{\text{PS},i}$ denote the number of phase shifters connected to a single RF chain in the i_{th} subarray. For the above parameters, we have following equations.

$$N_{\text{RF}} = \sum_{i=1}^{N_{\text{sub}}} N_{\text{RF},i}, \quad (5)$$

$$N_t = \sum_{i=1}^{N_{\text{sub}}} N_{t,i}, \quad (6)$$

$$N_{\text{PS}} = \sum_{i=1}^{N_{\text{sub}}} N_{\text{PS},i} N_{\text{RF},i}. \quad (7)$$

Moreover, the following inequality relations should also be satisfied, which can be presented as

$$1 \leq N_{\text{RF},i} \leq N_{t,i} = N_{\text{PS},i}, \quad (8)$$

$$N_{\text{sub}} \leq N_{\text{RF}} \leq N_t \leq N_{\text{PS}}, \quad (9)$$

where (8) is an obvious conclusion, and (9) can be proved as

$$N_{\text{RF}} = \sum_{i=1}^{N_{\text{sub}}} N_{\text{RF},i} \geq \sum_{i=1}^{N_{\text{sub}}} 1 = N_{\text{sub}}, \quad (10)$$

$$N_t = \sum_{i=1}^{N_{\text{sub}}} N_{t,i} \geq \sum_{i=1}^{N_{\text{sub}}} N_{\text{RF},i} = N_{\text{RF}}, \quad (11)$$

$$N_{\text{PS}} = \sum_{i=1}^{N_{\text{sub}}} N_{\text{PS},i} N_{\text{RF},i} = \sum_{i=1}^{N_{\text{sub}}} N_{t,i} N_{\text{RF},i} \geq \sum_{i=1}^{N_{\text{sub}}} N_{t,i} = N_t. \quad (12)$$

For any given RF and antenna mappings, the analog precoding matrix \mathbf{F}_{RF} is a block diagonal matrix, which can be expressed as

$$\mathbf{F}_{\text{RF}} = \begin{bmatrix} \mathbf{F}_{\text{RF},1} & & & \\ & \mathbf{F}_{\text{RF},2} & & \\ & & \ddots & \\ & & & \mathbf{F}_{\text{RF},N_{\text{sub}}} \end{bmatrix}, \quad (13)$$

where $\mathbf{F}_{\text{RF},i} = [\mathbf{a}_{i,1}, \mathbf{a}_{i,2}, \dots, \mathbf{a}_{i,N_{\text{RF},i}}]$, $i = 1, 2, \dots, N_{\text{sub}}$, and $\mathbf{a}_{i,j}$ of size $N_{t,i} \times 1$ is the analog precoding vector for the j_{th} RF chain in the i_{th} subarray. All the non-zero elements of $\mathbf{F}_{\text{RF},i}$ should satisfy the constant modulus constraint since the analog precoding is implemented utilizing analog phase shifters, i.e., $|\mathbf{F}_{\text{RF},i}(\cdot, \cdot)| = 1/\sqrt{N_{t,i}}$. Moreover, the digital precoding matrix \mathbf{F}_{BB} is also a block diagonal matrix, i.e.,

$$\mathbf{F}_{\text{BB}} = \begin{bmatrix} \mathbf{F}_{\text{BB},1} & & & \\ & \mathbf{F}_{\text{BB},2} & & \\ & & \ddots & \\ & & & \mathbf{F}_{\text{BB},N_{\text{sub}}} \end{bmatrix}, \quad (14)$$

where $\mathbf{F}_{\text{BB},i} = [\mathbf{d}_{i,1}; \mathbf{d}_{i,2}; \dots; \mathbf{d}_{i,N_{\text{sub}}}]$, $i = 1, 2, \dots, N_{\text{RF},i}$ is used to cancel the interference and allocate power for the data streams on the i_{th} subarray and $\mathbf{d}_{i,j}$ is a $1 \times N_{\text{RF},i}$ digital precoding vector. Note that $N_s = N_{\text{RF}}$ is assumed. To simplify the expression, we denote by $\mathbf{F} = \mathbf{F}_{\text{RF}}\mathbf{F}_{\text{BB}}$ the hybrid precoding matrix in the rest of paper. It could be observed that \mathbf{F} is block diagonal.

B. SIC-based hybrid precoding with arbitrary RF and antenna mappings

We aim to design the analog precoding matrix \mathbf{F}_{RF} and the digital precoding matrix \mathbf{F}_{BB} to maximize the total achievable rate R , which can be expressed as

$$\mathbf{F}^{\text{opt}} = \arg \max_{\mathbf{F}} R, \quad (15)$$

where

$$R = \log_2 \left(\left| \mathbf{I}_{N_r} + \frac{\rho}{N_s \sigma^2} \mathbf{H} \mathbf{F} \mathbf{F}^* \mathbf{H}^* \right| \right). \quad (16)$$

Since the non-convex constraints on the analog precoding matrix \mathbf{F}_{RF} , it is very difficult to obtain the globally optimal solution to (15). However, considering that the hybrid precoding matrix \mathbf{F} is of block diagonal structure, which means the precoding on each subarray is mutually independent, the total achievable rate R could be decomposed into multiple sub-rates, each of which is only related to one subarray. Then, we could solve (15) through maximize each sub-rate.

Note that when $N_{\text{sub}}=1$, this is actually the full-connected architecture, therefore, we only consider cases when $N_{\text{sub}} > 1$. The hybrid precoding matrix \mathbf{F} could be divided as

$$\mathbf{F} = \begin{cases} \begin{bmatrix} \hat{\mathbf{f}}_{N_{\text{sub}}-1} \mathbf{f}_{N_{\text{sub}}} \end{bmatrix}, & \text{if } N_{\text{RF}} = N_{\text{sub}} = 2, \\ \begin{bmatrix} \hat{\mathbf{F}}_{N_{\text{sub}}-1} \mathbf{f}_{N_{\text{sub}}} \end{bmatrix}, & \text{if } N_{\text{RF},N_{\text{sub}}} = 1, N_{\text{RF}} > 2, \\ \begin{bmatrix} \hat{\mathbf{f}}_{N_{\text{sub}}-1} \mathbf{F}_{N_{\text{sub}}} \end{bmatrix}, & \text{if } N_{\text{RF},N_{\text{sub}}} = N_{\text{RF}} - 1 > 1, \\ \begin{bmatrix} \hat{\mathbf{F}}_{N_{\text{sub}}-1} \mathbf{F}_{N_{\text{sub}}} \end{bmatrix}, & \text{others,} \end{cases} \quad (17)$$

where $\mathbf{f}_{N_{\text{sub}}}$ or $\mathbf{F}_{N_{\text{sub}}}$ are the last $N_{\text{RF},N_{\text{sub}}}$ columns of \mathbf{F} , and $\hat{\mathbf{f}}_{N_{\text{sub}}-1}$ or $\hat{\mathbf{F}}_{N_{\text{sub}}-1}$ denote the first $N_{\text{sub}}-1$ hybrid precoders. We then take the case presented in (20) as an example to introduce the rate decomposition processes and the corresponding operations for other cases can be carried out in the similar way. The total achievable rate R can be

rewritten as

$$\begin{aligned} R &= \log_2 \left(\left| \mathbf{I}_{N_r} + \frac{\rho}{N_s \sigma^2} \mathbf{H} \mathbf{F} \mathbf{F}^* \mathbf{H}^* \right| \right) \\ &= \log_2 \left(\left| \mathbf{I}_{N_r} + \frac{\rho}{N_s \sigma^2} \mathbf{H} \left[\hat{\mathbf{F}}_{N_{\text{sub}}-1} \mathbf{F}_{N_{\text{sub}}} \right] \left[\hat{\mathbf{F}}_{N_{\text{sub}}-1} \mathbf{F}_{N_{\text{sub}}} \right]^* \mathbf{H}^* \right| \right) \\ &\stackrel{(a)}{=} \log_2 \left(\left| \mathbf{I}_{N_r} + \frac{\rho}{N_s \sigma^2} \mathbf{H} \hat{\mathbf{F}}_{N_{\text{sub}}-1} \hat{\mathbf{F}}_{N_{\text{sub}}-1}^* \mathbf{H}^* \right. \right. \\ &\quad \left. \left. + \frac{\rho}{N_s \sigma^2} \mathbf{H} \mathbf{F}_{N_{\text{sub}}} \mathbf{F}_{N_{\text{sub}}}^* \mathbf{H}^* \right| \right) \\ &\stackrel{(b)}{=} \log_2 (|\mathbf{C}_{N_{\text{sub}}-1}|) \\ &\quad + \log_2 \left(\left| \mathbf{I}_{N_r} + \frac{\rho}{N_s \sigma^2} \mathbf{C}_{N_{\text{sub}}-1}^{-1} \mathbf{H} \mathbf{F}_{N_{\text{sub}}} \mathbf{F}_{N_{\text{sub}}}^* \mathbf{H}^* \right| \right) \\ &\stackrel{(c)}{=} \log_2 (|\mathbf{C}_{N_{\text{sub}}-1}|) \\ &\quad + \log_2 \left(\left| \mathbf{I}_{N_{\text{RF},N_{\text{sub}}}} + \frac{\rho}{N_s \sigma^2} \mathbf{F}_{N_{\text{sub}}}^* \mathbf{H}^* \mathbf{C}_{N_{\text{sub}}-1}^{-1} \mathbf{H} \mathbf{F}_{N_{\text{sub}}} \right| \right) \\ &\stackrel{(d)}{=} \sum_{i=1}^{N_{\text{sub}}} \log_2 \left(\left| \mathbf{I}_{N_{\text{RF},i}} + \frac{\rho}{N_s \sigma^2} \mathbf{F}_i^* \mathbf{H}^* \mathbf{C}_{i-1}^{-1} \mathbf{H} \mathbf{F}_i \right| \right), \end{aligned} \quad (21)$$

where $\mathbf{C}_{N_{\text{sub}}-1} = \mathbf{I}_{N_r} + \frac{\rho}{N_s \sigma^2} \mathbf{H} \hat{\mathbf{F}}_{N_{\text{sub}}-1} \hat{\mathbf{F}}_{N_{\text{sub}}-1}^* \mathbf{H}^*$, $\mathbf{C}_0 = \mathbf{I}_{N_{\text{RF},1}}$. (a) is obtained since the hybrid precoding matrix \mathbf{F} is of block diagonal structure and the precoders for different subarrays are diagonal. Step (b) is true due to the fact that $|\mathbf{A}\mathbf{B}| = |\mathbf{A}||\mathbf{B}|$ and let $\mathbf{A} = \log_2 (|\mathbf{C}_{N_{\text{sub}}-1}|)$, $\mathbf{B} = \log_2 \left(\left| \mathbf{I}_{N_r} + \frac{\rho}{N_s \sigma^2} \mathbf{C}_{N_{\text{sub}}-1}^{-1} \mathbf{H} \mathbf{F}_{N_{\text{sub}}} \mathbf{F}_{N_{\text{sub}}}^* \mathbf{H}^* \right| \right)$. (c) is obtained due to the fact that $|\mathbf{I} + \mathbf{A}\mathbf{B}| = |\mathbf{I} + \mathbf{B}\mathbf{A}|$ by defining $\mathbf{A} = \mathbf{C}_{N_{\text{sub}}-1}^{-1} \mathbf{H} \mathbf{F}_{N_{\text{sub}}}$ and $\mathbf{B} = \mathbf{F}_{N_{\text{sub}}}^* \mathbf{H}^*$. Note that, the second term $\log_2 \left(\left| \mathbf{I}_{N_{\text{RF},N_{\text{sub}}}} + \frac{\rho}{N_s \sigma^2} \mathbf{F}_{N_{\text{sub}}}^* \mathbf{H}^* \mathbf{C}_{N_{\text{sub}}-1}^{-1} \mathbf{H} \mathbf{F}_{N_{\text{sub}}} \right| \right)$ of step (c) is the achievable sub-rate for the $(N_{\text{sub}})_{th}$ subarray and the form of the first term $\log_2 (|\mathbf{C}_{N_{\text{sub}}-1}|)$ is similar as (16). This observation implies that we can further decompose $\log_2 (|\mathbf{C}_{N_{\text{sub}}-1}|)$ utilizing the similar method in (21). Step (d) is the result after N_{sub} decompositions.

As has shown in (21), the total achievable rate R is the sum of sub-rates for all the subarrays. Therefore, the total optimization problem (16) can be transformed into a series of sub-rate optimization problems of subarrays, which can be solved one by one. Similar as [8], we adopt the idea of SIC to optimize the multiple sub-rates. The sub-rate optimization problem for the i_{th} subarray can be stated as

$$\mathbf{F}_i^{\text{opt}} = \arg \max_{\mathbf{F}_i} \log_2 \left(\left| \mathbf{I}_{N_{\text{RF},i}} + \frac{\rho}{N_s \sigma^2} \mathbf{F}_i^* \mathbf{P}_{i-1} \mathbf{F}_i \right| \right), \quad (22)$$

where $\mathbf{P}_{i-1} = \mathbf{H}^* \mathbf{C}_{i-1}^{-1} \mathbf{H}$ is $N_t \times N_t$ Hermitian matrix. Note that only elements from the $A = (\sum_{j=1}^{i-1} N_{t,j} + 1)_{th}$ row to the $B = (\sum_{j=1}^i N_{t,j})_{th}$ row in the i_{th} precoder \mathbf{F}_i are non-zero ($N_{t,0}$ is set to be 0). Therefore, the sub-rate optimization problem (22) can be written as

$$\tilde{\mathbf{F}}_i^{\text{opt}} = \arg \max_{\tilde{\mathbf{F}}_i} \log_2 \left(\left| \mathbf{I}_{N_{\text{RF},i}} + \frac{\rho}{N_s \sigma^2} \tilde{\mathbf{F}}_i^* \tilde{\mathbf{P}}_{i-1} \tilde{\mathbf{F}}_i \right| \right), \quad (23)$$

where $\tilde{\mathbf{F}}_i$ of size $N_{t,i} \times N_{\text{RF},i}$ is the sub-matrix of \mathbf{F}_i from the A_{th} row to the B_{th} row, $\tilde{\mathbf{P}}_{i-1}$ of size $N_{t,i} \times N_{t,i}$ is the sub-matrix of \mathbf{P}_{i-1} from the A_{th} row and column to the B_{th} row

and column. Define the singular value decomposition (SVD) of the Hermitian matrix $\tilde{\mathbf{P}}_{i-1}$ as

$$\tilde{\mathbf{P}}_{i-1} = \mathbf{V}_{i-1} \mathbf{\Sigma}_{i-1} \mathbf{V}_{i-1}^*, \quad (24)$$

where $\mathbf{\Sigma}_{i-1}$ is a diagonal matrix containing the singular values of $\tilde{\mathbf{P}}_{i-1}$ in the decreasing order and \mathbf{V}_{i-1} is a unitary matrix of size $N_{t,i} \times N_{t,i}$. It is known that the unconstrained precoding matrix of the i_{th} subarray is the first $N_{RF,i}$ columns of \mathbf{V}_{i-1} , i.e.,

$$\tilde{\mathbf{f}}_i^{\text{opt}} = \mathbf{V}_{i-1}(:, 1:N_{RF,i}). \quad (25)$$

The total unconstrained precoding matrix \mathbf{F}^{opt} is the block diagonal concatenation of $\tilde{\mathbf{f}}_i^{\text{opt}}$ and can be obtained through N_{sub} iterations, which can be presented as

$$\mathbf{F}^{\text{opt}} = \begin{bmatrix} \tilde{\mathbf{f}}_1^{\text{opt}} & & & \\ & \tilde{\mathbf{f}}_2^{\text{opt}} & & \\ & & \ddots & \\ & & & \tilde{\mathbf{f}}_{N_{\text{sub}}}^{\text{opt}} \end{bmatrix}. \quad (26)$$

Since there are constant modulus constrains on the elements of analog precoding matrix \mathbf{F}_{RF} , we cannot directly set \mathbf{F}^{opt} as the solution to the optimization problem (15). To obtain a practical solution, we try to further convert (23).

Lemma 1: When $N_{RF,i} = 1$, the optimization problem (23) can be rewritten as

$$\tilde{\mathbf{f}}_i^{\text{opt}} = \arg \max_{\tilde{\mathbf{f}}_i} \log_2 \left(\left| \mathbf{I}_{N_{RF,i}} + \frac{\rho}{N_s \sigma^2} \tilde{\mathbf{f}}_i^* \tilde{\mathbf{P}}_{i-1} \tilde{\mathbf{f}}_i \right| \right), \quad (27)$$

which is equivalent to

$$\tilde{\mathbf{f}}_i^{\text{opt}} = \arg \max_{\tilde{\mathbf{f}}_i} \left\| \mathbf{v}_{i-1} - \tilde{\mathbf{f}}_i \right\|_2^2, \quad (28)$$

where \mathbf{v}_i is the first right singular vector of $\hat{\mathbf{P}}_{i-1}$.

Proof 1: See Appendix A in [8].

The solution to (28) can be easily given as

$$\mathbf{a}_i = \frac{1}{\sqrt{N_{t,i}}} \exp(j \angle(\mathbf{v}_{i-1})), \quad (29)$$

$$\mathbf{d}_i = \frac{\|\mathbf{v}_{i-1}\|_1}{\sqrt{N_{t,i}}}, \quad (30)$$

$$\tilde{\mathbf{f}}_i = \frac{1}{N_{t,i}} \|\mathbf{v}_{i-1}\|_1 \exp(j \angle(\mathbf{v}_{i-1})). \quad (31)$$

Lemma 2: When $N_{RF,i} > 1$, the optimization problem (24) is equivalent to

$$\tilde{\mathbf{F}}_i^{\text{opt}} = \arg \max_{\tilde{\mathbf{F}}_i} \left\| \mathbf{V}_{i-1}(:, 1:N_{RF,i}) - \tilde{\mathbf{F}}_i \right\|_F^2, \quad (32)$$

Proof 2: The proof are similar as the formula deduction process in Section III of [6] and thus is omitted.

Corollary 1: Similar as the idea to solve (28), the practical analog/digital precoding matrices of (32) can be obtained by

$$\mathbf{F}_{\text{RF},i} = \frac{1}{\sqrt{N_{t,i}}} \exp(j \angle(\mathbf{V}_{i-1}(:, 1:N_{RF,i}))), \quad (33)$$

Algorithm 1 Hybrid Precoding For Arbitrary Antenna and RF Mappings in the Extended Sub-connected Structure

Initialization: \mathbf{H} , N_{RF} , $N_{\text{RF},i}$, $N_{t,i}$, $i = 1, 2, \dots, N_{\text{sub}}$

Output: The total hybrid precoding matrix \mathbf{F}

```

1:  $\mathbf{P} = \mathbf{H}^* \mathbf{H}$ 
2: for  $i \leq N_{\text{sub}}$  do
3:    $\tilde{\mathbf{P}} = \mathbf{V} \mathbf{\Sigma} \mathbf{V}^*$ 
4:   if  $N_{\text{RF},i} == 1$  then
5:      $\mathbf{a}_i = \frac{1}{\sqrt{N_{t,i}}} \exp(j \angle(\mathbf{v}_{i-1}))$ ,  $\mathbf{d}_i = \frac{\|\mathbf{v}_{i-1}\|_1}{\sqrt{N_{t,i}}}$ 
6:      $\tilde{\mathbf{f}}_i = \frac{1}{N_{t,i}} \|\mathbf{v}_{i-1}\|_1 \exp(j \angle(\mathbf{v}_{i-1}))$ 
7:   else
8:      $\mathbf{F}_{\text{RF},i} = \frac{1}{\sqrt{N_{t,i}}} \exp(j \angle(\mathbf{V}(:, 1:N_{\text{RF},i})))$ 
9:      $\mathbf{F}_{\text{BB},i} = (\mathbf{F}_{\text{RF},i}^* \mathbf{F}_{\text{RF},i})^{-1} \mathbf{F}_{\text{RF},i}^* \mathbf{V}(:, 1:N_{\text{RF},i})$ 
10:     $\tilde{\mathbf{F}}_i = \mathbf{F}_{\text{RF},i} \mathbf{F}_{\text{BB},i}$ 
11:   end if
12:   if  $i == 1$  and  $N_{\text{RF},1} == 1$  then
13:      $\mathbf{C}_i = \mathbf{I}_{N_r} + \frac{\rho}{N_s \sigma^2} \mathbf{H} \tilde{\mathbf{f}}_i \tilde{\mathbf{f}}_i^* \mathbf{H}^*$ 
14:   else
15:      $\mathbf{C}_i = \mathbf{I}_{N_r} + \frac{\rho}{N_s \sigma^2} \mathbf{H} \tilde{\mathbf{F}}_i \tilde{\mathbf{F}}_i^* \mathbf{H}^*$ 
16:   end if
17:   Update  $\mathbf{P} = \mathbf{H}^* \mathbf{C}_i^{-1} \mathbf{H}$ 
18: end for
19: Construct  $\mathbf{F}$  as (37)

```

$$\mathbf{F}_{\text{BB},i} = (\mathbf{F}_{\text{RF},i}^* \mathbf{F}_{\text{RF},i})^{-1} \mathbf{F}_{\text{RF},i}^* \mathbf{V}_{i-1}(:, 1:N_{\text{RF},i}), \quad (34)$$

$$\tilde{\mathbf{F}}_i = \mathbf{F}_{\text{RF},i} \mathbf{F}_{\text{BB},i}. \quad (35)$$

Proof 3: The proof is omitted due to space limitation.

After we solve all sub-rate optimization problems for all subarrays with if $N_{\text{RF},1} = 1$ or if $N_{\text{RF},1} > 1$ RF chains. The total practical hybrid precoding matrix can be presented as

$$\mathbf{F} = \begin{bmatrix} \tilde{\mathbf{F}}_1, & \text{if } N_{\text{RF},1} > 1 \\ & \ddots \\ & & \tilde{\mathbf{f}}_i, & \text{if } N_{\text{RF},i} = 1 \\ & & & \ddots \\ & & & & \tilde{\mathbf{F}}_j, & \text{if } N_{\text{RF},j} > 1 \\ & & & & & \ddots \\ & & & & & & \tilde{\mathbf{f}}_{N_{\text{sub}}}, & \text{if } N_{\text{RF},N_{\text{sub}}} = 1 \end{bmatrix}. \quad (36)$$

As has described above, the total achievable rate is decomposed into series sub-rates and the total optimizing problem (15) is correspondingly decomposed into multiple sub-rate optimizing problems, each of which is only related to one subarray. All above details are summarized in **Algorithm 1**.

C. Energy efficiency

For millimeter wave MIMO systems with hybrid precoding architecture, the energy efficiency can be defined as the ratio between achievable rate and total power consumption [7], i.e.,

$$\eta = \frac{R}{P_{\text{total}}} = \frac{R}{P_{\text{CO}} + N_{\text{RF}} P_{\text{RF}} + N_t P_{\text{PA}} + N_{\text{PS}} P_{\text{PS}}}, \quad (37)$$

where P_{CO} is the common power of the transmitter including site-cooling, baseband processing and synchronization. P_{RF} ,

P_{PA} , and P_{PS} are the power of each RF chain, phase shifter and power amplifier, respectively. Note that, N_t and N_{RF} are constants, only N_{PS} is a variable. The numbers of phase shifters for the full-connected architecture, sub-connected architecture and the extended sub-connected architecture are summarized as follows.

$$N_{PS} = \begin{cases} N_t N_{RF}, & \text{Full-connected,} \\ N_t, & \text{Sub-connected,} \\ \sum_{i=1}^{N_{sub}} N_{PS,i} N_{RF,i}, & \text{Extended sub-connected,} \end{cases} \quad (38)$$

$$(39)$$

$$(40)$$

which satisfy the following inequality as

$$N_t \leq \sum_{i=1}^{N_{sub}} N_{PS,i} N_{RF,i} \leq N_t N_{RF}, \quad (41)$$

where the first inequality has been given in (12) and the second inequality is given by

$$\sum_{i=1}^{N_{sub}} N_{PS,i} N_{RF,i} = \sum_{i=1}^{N_{sub}} N_{t,i} N_{RF,i} \leq \sum_{i=1}^{N_{sub}} N_{t,i} N_{RF} = N_t N_{RF}. \quad (42)$$

Therefore, we can conclude that $P_{total}^{Sub} \leq P_{total}^{Extended} \leq P_{total}^{Full}$.

Moreover, to simplify the analysis, we assume the number of antennas connected to a subarray is proportional to the corresponding number of RF chains in this subarray, i.e.,

$$N_{t,i} = \frac{N_t}{N_{RF}} N_{RF,i}. \quad (43)$$

Then, we could directly obtain

$$\frac{N_t}{N_{RF}} \leq N_{t,i} \leq N_t. \quad (44)$$

Generally, the more number of antennas connected to each RF chain, the higher the achievable rate is. Therefore, in terms of achievable rate, we have $R^{Sub} \leq R^{Extended} \leq R^{Full}$.

Based on the above analysis, we could find that the full-connected architecture enjoys highest achievable rate but also causes the most power consumption and the sub-connected architecture needs the least power consumption but sacrifices many achievable rates. Due to the nonlinear dependence of energy efficiency on the number of data streams, RF chains and antennas, the architecture with highest energy efficiency is theoretically unknown. Therefore, we provide a variety of numerical comparisons in Section IV, which demonstrate that the extended sub-connected architecture could achieve the best energy efficiency compares with the existing full-connected and sub-connected architectures.

IV. SIMULATION RESULTS

In this section, the performances of the proposed scheme (marked as Extended-SIC) are evaluated. We adopt the OMP scheme in the full-connected architecture [6] and the SIC based scheme in the sub-connected architecture (marked as Split-SIC) [8] as the benchmarks. The unconstrained precoding scheme (marked as Extended-opt) for the extended sub-connected architecture is given in (26). Moreover, the situation that the numbers of RF chains in different subarrays are the

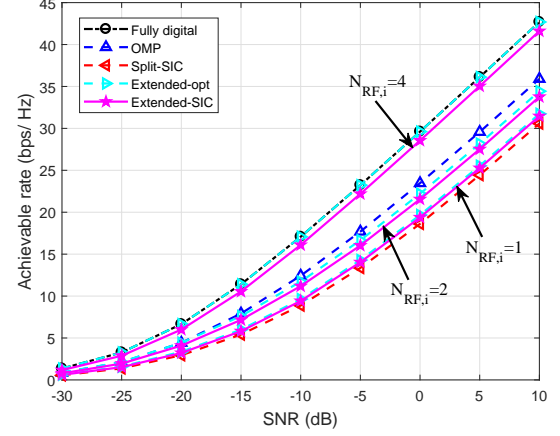


Fig. 2. Achievable rate vs SNR with $N_t = 144$, $N_r = 36$ and $N_{RF} = 4$.

same is specially marked out as “Extended-SIC-equal-RF”. Both the transmitter and the receiver are equipped with ULAs with $\lambda/2$ aperture domain sample spacing. Moreover, the channel parameters are set as $N_{cl} = 10$ and $N_{ray} = 5$. The azimuth AOAs and AODs follow the Laplacian distribution with uniformly distributed mean angles within $(0, 2\pi]$ and angular spread of 7.5° [6]. The power consumptions for different hardware as set as follows: $P_{CO} = 10W$, $P_{RF} = 100mW$, $P_{PA} = 100mW$, $P_{PS} = 10mW$ [10]. Finally, the signal-to-noise ratio (SNR) is defined as $\frac{P}{\sigma^2}$.

Fig. 2 shows the achievable rates of the proposed Extended-SIC scheme, Extended-opt scheme, OMP scheme and Split-SIC scheme, where $N_t = 144$, $N_r = 36$, $N_{RF} = 4$ and we assume $N_{RF,1} = \dots = N_{RF,N_{sub}} = N_{RF,i}$. When $N_{RF,i} = 1$, the extended sub-connected architecture is just the traditional sub-connected architecture, we could observe that the achievable rate of proposed Extended-SIC scheme is similar as (little larger than) the Split-SIC scheme. When $N_{RF,i} = 4$, which means there is only one subarray, the extended sub-connected architecture is now the full-connected architecture. It can be observed that the unconstrained precoding scheme and the Extended-SIC scheme obtain nearly the same achievable rate as the fully digital scheme. When $N_{RF,i} = 2$, we can observe that the proposed Extended-SIC scheme still achieves similar achievable rate as the OMP scheme.

Fig. 3 show the achievable rate with different numbers of antennas at the transmitter, when $N_r = 36$, $N_s = N_{RF} = 8$. We compare different RF and antenna mappings, which are stated as (7, 1), (6, 1, 1), (5, 2, 1), (4, 4), (3, 3, 2) and (2, 2, 2, 2). For example, the mapping (5, 2, 1) means that there are 3 subarrays and the numbers of RF chains connected to the subarrays are 5, 2 and 1, respectively. At the same time, according to (43), the corresponding numbers of antennas connected to subarrays are 5, 2 and 1 times of N_t/N_{RF} . Please note that, the proposed hybrid precoding scheme under mappings (4, 4) and (2, 2, 2, 2) are actually the scheme “Extended-SIC-equal-RF” mentioned above. It could be observed that, in terms of achievable rate, $R_{(7,1)} > R_{(6,1,1)} > R_{(5,2,1)} > R_{(4,4)} > R_{(3,3,2)} > R_{(2,2,2,2)} > R_{Split-SIC}$. Specially, we could observe that the achievable rate of the

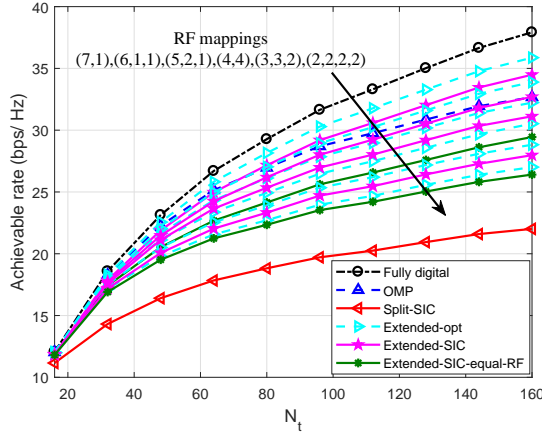


Fig. 3. Achievable rate vs N_t , with $N_r = 36$, $N_s = N_{RF} = 8$.

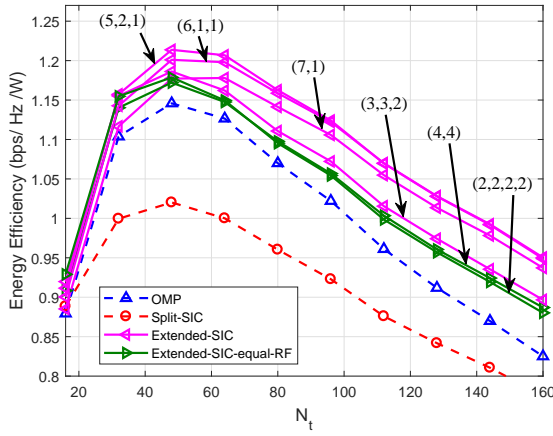


Fig. 4. Energy efficiency vs N_t with $N_r = 36$, $N_s = N_{RF} = 8$.

proposed Extended-SIC scheme in the extended sub-connected architecture under the mapping (5, 2, 1) is similar as the OMP scheme in the full-connected architecture.

Fig. 4 compares the energy efficiency of different schemes for different numbers of antennas at the transmitter. The system parameters are set the same as that in Fig. 3. It could be observed that the Extended-SIC scheme in extended sub-connected architectures with the given mappings are always the best compared with the schemes in full-connected the sub-connected architectures. As for the peak values of energy efficiencies, the mapping (5, 2, 1) is the best. In addition, the mappings (7, 1), (6, 1, 1) and (5, 2, 1) are better than (4, 4) and (2, 2, 2, 2), where the energy efficiencies for mappings (4, 4) and (2, 2, 2, 2) are nearly the same. Furthermore, it could also be observed that, the energy efficiencies of all schemes increase first and then decrease as the number of antennas increases. For the considered system parameters (i.e., $N_r = 36$, $N_s = N_{RF} = 8$), the energy efficiency is highest when the number of antennas is about 48.

V. CONCLUSIONS

In this paper, an extended sub-connected architecture with arbitrary RF and antenna mappings was proposed to improve

the energy efficiency of the hybrid precoding in millimeter wave MIMO systems. For any given RF and antenna mappings, we proposed a SIC-based hybrid precoding scheme with near-optimal performance. A variety of results were exhibited by changing RF and antennas mappings to provide references for the design of better energy efficient architecture. Simulation results verified that the proposed scheme in the extended sub-connected architecture achieves similar achievable rate as the corresponding unconstrained optimal precoding scheme and achieves the best energy-efficiency performance compared with the existing schemes in the full-connected and sub-connected architectures.

REFERENCES

- [1] C. X. Wang, F. Haider, X. Gao, X. H. You, Y. Yang, D. Yuan, H. M. Aggoune, H. Haas, S. Fletcher, and E. Hepsaydir, "Cellular architecture and key technologies for 5G wireless communication networks," *IEEE Commun. Mag.*, vol. 52, no. 2, pp. 122-130, Feb. 2014.
- [2] R. W. Heath, N. Gonzalez-Prelcic, S. Rangan, W. Roh and A. M. Sayeed, "An overview of signal processing techniques for millimeter wave MIMO systems," *IEEE J. Sel. Areas Commun.*, vol. 10, no. 3, pp. 436-453, Apr. 2016.
- [3] P. Liu, S. Jin, T. Jiang, Q. Zhang, and M. Matthaiou, "Pilot power allocation through user grouping in multi-cell massive MIMO systems," *IEEE Trans. Commun.*, vol. 65, no. 4, pp. 1561-1574, Apr. 2017.
- [4] S. Qiu, Da Chen, D. Qu, K. Luo and T. Jiang, "Downlink precoding with mixed statistical and imperfect instantaneous CSI for massive MIMO systems," *IEEE Trans. Veh. Technol.*, vol. 67, no. 4, pp. 3028-3041, Apr. 2018.
- [5] T. Zhang, C. Wen, S. Jin, and T. Jiang, "Mixed-ADC massive MIMO detectors: performance analysis and design optimization," *IEEE Trans. Wireless Commun.*, vol. 15, no. 11, pp. 7738-7752, Nov. 2016.
- [6] O. E. Ayach, S. Rajagopal, S. Abu-Surra, Z. Pi, and R. W. Heath, Jr, "Spatially sparse precoding in millimeter wave MIMO systems," *IEEE Trans. Wireless Commun.*, vol. 13, no. 3, pp. 1499-1513, Mar. 2014.
- [7] X. Yu, J.-C. Shen, J. Zhang, and K. B. Letaief, "Alternating minimization algorithms for hybrid precoding in millimeter wave MIMO systems," *IEEE J. Sel. Topics Signal Process.*, vol. 10, no. 3, pp. 485-500, Apr. 2016.
- [8] X. Gao, L. Dai, S. Han, I. Chih-Lin, and R. W. Heath, "Energy-efficient hybrid analog and digital precoding for mmWave MIMO systems with large antenna arrays," *IEEE J. Sel. Areas Commun.*, vol. 34, no. 4, pp. 998-1009, Apr. 2016.
- [9] D. Zhang, Y. Wang, X. Li, W. Xiang, "Hybridly-Connected Structure for Hybrid Beamforming in mmWave Massive MIMO Systems," *IEEE Trans. Commun.*, vol. 66, no. 2, pp. 662-674, Feb. 2018.
- [10] P. Netrapalli, P. Jain, and S. Sanghavi, "Phase retrieval using alternating minimization," *IEEE Trans. Signal Process.*, vol. 63, no. 18, pp. 4814-4826, Sep. 2015.